Japanese Journal of Applied Physics **50** (2011) 040206 **RAPID COMMUNICATION**
DOI: 10.1143/JJAP.50.040206

Enhanced Properties in Single-Walled Carbon Nanotubes Based Saturable Absorber for All Optical Signal Regeneration

Hanond Nong*, Maud Gicquel-Guézo, Laurent Bramerie, Mathieu Perrin, Frédéric Grillot, Romain Fleurier[1], Baolai Liang[2], Diana L. Huffaker[2], Christophe Levallois, Julie Le Pouliquen, Alain Le Corre, Olivier Dehaese, and Slimane Loualiche

Université Européenne de Bretagne, CNRS — Laboratoire FOTON UMR 6082 — INSA Rennes, 20 avenue des Buttes de Coësmes, 35708 Rennes Cedex 7, France
[1]*Laboratoire d'Etude des Microstructures, ONERA–CNRS, 29 Avenue de la division Leclerc, 92322 Châtillon Cedex, France*
[2]*Electrical Engineering Department, Engineering IV 18-141, University of California at Los Angeles, Los Angeles, CA 90095, U.S.A.*

Received November 17, 2010; accepted January 28, 2011; published online April 5, 2011

Ultrafast relaxation dynamics of photogenerated carriers in nanostructure based saturable absorber (SA) are investigated using a degenerate cross-polarized pump–probe experiment at 1.55 μm operating wavelength. Single-walled carbon nanotubes (SWNT) encased in micelles are studied and compared to bundled ones as well as to iron doped InGaAs/InP multiple quantum wells (MQW). SA parameters for all optical signal regeneration (AOSR) are extracted from the normalized differential transmission. Although all samples show the same order of recombination time, SWNT in micelles present a much higher contrast ratio associated to a lower level of saturation fluence as compared to their bundled and MQW counterparts.

According to the potential economical interest to increase the bit rate per channel in optical telecommunication systems, signal regeneration is required in order to counteract propagation impairments from loss, dispersion, noise and crosstalk. An alternative of the expensive cost of optoelectronic signal regeneration devices implementation, relies on the use of optical gates (2R regeneration) such as passive semiconductor saturable absorber devices (SA).[1)] When included in a telecom network, a SA microcavity reduces the noise amplitude of the logical '0' while enhancing the level of logical '1' through its optical nonlinear properties. However, in order to reduce the noise amplitude of logical '1', another SA is required and it can be made by properly choosing cavity parameters so as to obtain a reflectance curve decreasing with input power.[2)] The use of both SA microcavities in cascade leads to a significant reduction of the noise in a telecom system.[3)] Typical devices for 2R all-optical signal regeneration (AOSR) are based on doped multiple quantum wells (MQW). However realization of MQW based SA requires complex fabrication steps during the growth process so as to ensure an accurate control of both the wells thickness (related to the device absorption band) and the doping level (linked to the switching time and the saturation fluence[4)]).

A cheaper alternative of such semiconductor nanostuctures relies on the use of single-walled carbon nanotubes (SWNT), which have shown to possess faster intrinsic switching time dynamics especially in bundled configuration.[5–7)] SWNT have also a larger third-order susceptibility imaginary part[8)] (e.g., $|\mathrm{Im}\,\chi^{(3)}|$), which is linked to the variation of the absorption meaning that one can expect a relatively higher contrast ratio for SA based on SWNT. Recently pump–probe experiments have been conducted on bundled SWNT (B-SWNT) and compared to MQW based SA. Although the time dynamic relaxation has appeared much faster for SWNT (0.51 ps) as compared to MQWs (3.42 ps), results have shown that both saturation fluence and contrast need to be enhanced.[9)]

This letter aims to propose a SWNT configuration allowing to significantly enhance the SA properties of these materials. We show that SWNT in micelles environment lead to a much higher contrast ratio associated to a lower level of saturation fluence as compared to their bundled and MQW counterparts. These results suggest that efficient low cost saturable absorber can be achieved by using SWNT in preference to MQW.

The structural composition and optical linear absorption of Fe doped MQW and B-SWNT based SA have already been described elsewere.[9)] The third sample based SA consist in Mic-SWNT. HiPCO SWNT have been dispersed and sonicated in water with sodium cholate. Then it was centrifuged at 25 000g during one hour and the supernatant is dropped on a glass subtraste.

Figure 1(a) shows the absorption spectrum from B-SWNT compared to the one from Mic-SWNT deposit on glass substrate. Both samples have a strong background absorption but on the contrary of B-SWNT, Mic-SWNT exhibit pronounced fine structures and visible photoluminescence peaks[10)] even at room temperature [cf. Fig. 1(b)]. These results show a quite perfect stability of SWNT transition wavelengths and amplitudes, as no obvious shift from 77 to 295 K is observed. On the contrary to usual semi-conductor quantum wells, which show temperature dependence of their optical transitions, such stability properties are of first importance as it allows an insensitivity to the bits sequence pattern for the signal regeneration processing. Moreover, the comparison between these two spectra points out that the first inhomogeneous optical transition of semi-conducting SWNT (S_1)[11,12)] in micelles is blueshifted. As one S_1 transition peak of Mic-SWNT resonates at 1.55 μm, we believe that the micelles environment may lead to a higher $|\mathrm{Im}\,\chi^{(3)}|$ and so to a higher contrast ratio as compared to B-SWNT.

In order to evaluate the optical SA properties of these nano-materials, pump–probe experiments are performed at 1.55 μm in a transmission configuration with optical excitation and probe pulses originate from an optical parametric oscillator. Details of the experimental setup are described in ref. 9. All measurements are made in a same experimental run. We first compare the dynamics of the transient change of

*E-mail address: hanond.nong@insa-rennes.fr

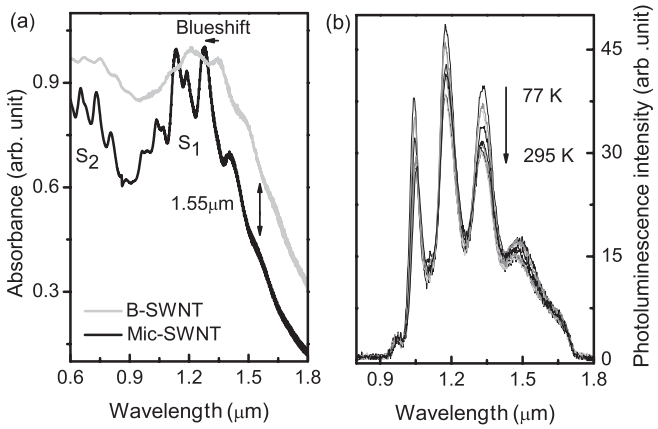

Fig. 1. (a) Optical transmission spectra of B-SWNT (grey line) and Mic-SWNT (dark line) deposited on glass sustrate, S_1 and S_2 denote first and second excitonic resonances of semi-conducting SWNT. The absorption blueshift is denoted by the black arrow. (b) Photoluminescence spectra of Mic-SWNT as a function of temperature (77 to 295 K) at same continuous excitation laser wavelength and intensity (0.65 μm and 10 mW, respectively). Note that photoluminescence peaks show remarkable stability to temperature variation.

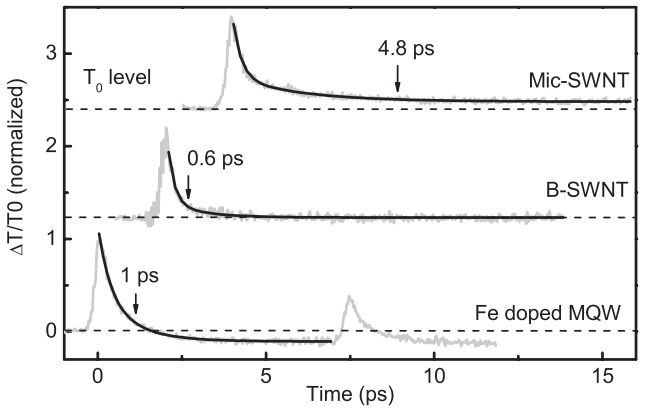

Fig. 2. Normalized NDT for Fe doped MQW InGaAs/InP in direct comparison with B-SWNT and Mic-SWNT HiPCO. Spectra were recorded in the same experimental run (grey lines), namely same incident pump fluence and wavelength (9 μJ·cm^{-2} and 1.55 μm, respectively). Decay times are obtained by curve-fitting (black lines). Black arrows denote the time before getting 90% of the recovery for the transient absorption. The saturation absorption dynamics is described by a bi-exponentional and time constants are summarized in Table I. Dash lines denote T_0 level.

Table I. Time constants of the bi-exponential curve-fitting.

Time constant (ps)	MQW	Bundled SWNT	Micelles SWNT
τ_1	0.37	0.18	0.25
τ_2	1	1	2

transmission for the three samples at the same input pump fluence of 9 μJ·cm^{-2} (cf. Fig. 2). In all cases the recombination profile is a bi-exponential decay (black lines, Fig. 2). Table I, in inset of Fig. 2, summarizes first and second time constants (τ_1 and τ_2, respectively) extracted from the absorption dynamics curve-fitting. The transient absorption dynamics of MQW presents two decay times corresponding to the excitons dissociation time followed by carriers capture through Fe atom traps.[13,14] The negative part of the NDT is attributed to photo-induced absorption due to the high doping level of the MQW nanostructures. This phenomenon can be observed for high-doped MQW when the number of photo-generated carriers, induced by the pumping in the nano-structure, is lower than the concentration of traps meaning that the level of saturation of the excitonic band does not compensate the photo-induced absorption due to re-excitation of trapped electron to the conduction band.[15] The second peak of transient transmission around 8 ps corresponds to the MQW re-excitation due to internal reflection at the interface. Concerning B-SWNT, the first decay time is attributed to the intraband decay in non-resonant SWNT and followed by a second time constant mainly governed by charge transfer from semiconducting to metallic SWNT through tunneling processes.[5] Dispersion and homogeneity of the deposit film being not well controlled, a small change in the absorption recovery time related to the probe's area onto the sample can be observed.

Mic-SWNT exhibit slower intraband decay with a second decay time mainly attributed to the interband relaxation in resonant SWNT.[6] As compared to MQW and B-SWNT, the overall recombination time remains much slower in Mic-SWNT compare to MQW and B-SWNT. More than 90% of the signal disappears within 4.8 ps (cf. Fig. 2) after pump excitation for Mic-SWNT (0.6 and 1 ps for B-SWNT and MQW, respectively). In this case, signal frequency up to 60 GHz can be regenerated with Mic-SWNT (time constant 3 times lower than the bit repetition rate). In order to improve the recovery time, the degree of aggregation of the tubes in Mic-SWNT clusters has to be enhanced. Consequently, a degradation of the nonlinear amplitude response occurs meaning that, depending on the targeted application, a trade off between amplitude and time responses have to be determined. Nevertheless, all of these dynamic times remain within the same order of magnitude. These results indicate that the micelles environment does not alter significantly the fast intrinsic switching response of SWNT.

In addition of an ultrafast absorption time recovery, two other important parameters are required for optimized AOSR. On the one hand, the saturation amplitude (contrast ratio in NDT) needs to be as high as possible because it is linked to the bit error rate (BER) parameter. The BER allows to evaluate the system performance and is proportional to $Q^{-1}\exp(-Q^2/2)$, where $Q = (I_1 - I_0)/(\sigma_1 + \sigma_0)$ with $I_1(I_0)$ and $\sigma_1(\sigma_0)$ are the mean amplitude and standard deviation values of 1 and 0 optical symbols respectively. The NDT is directly linked to the Q-factor since it contributes to increase the contrast $(I_1 - I_0)$ term. On the other hand, the saturation fluence needs to be as low as possible since it corresponds to the input fluence required for inducing switching phenomenon. In a transmission configuration both parameters can be determined by curve-fitting the excitation intensity dependence with the transient maximum NDT. Figure 3 shows experimental data adjusted with a semi-empirical absorption saturation relationship based on a two energy level system:[16] $\Delta T/T_0 = \exp[A/(1 + SF/F)] - 1$, where A is the absorbance of the sample, F is the excitation fluence and SF the saturation fluence. Experiments are made on the three samples and concerning Mic-SWNT, two areas

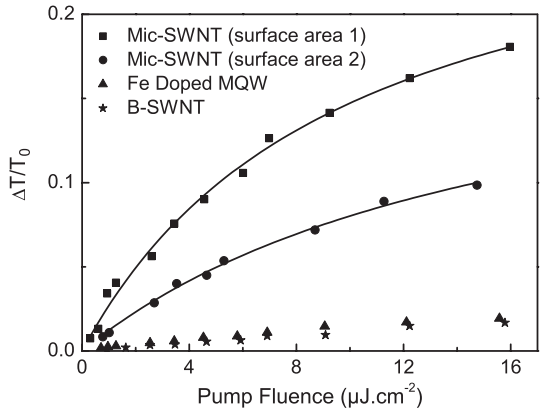

Fig. 3. NDT for Fe doped MQW, B-SWNT and Mic-SWNT as a function of input pump fluence at excitation wavelength of 1.55 μm. Using the saturation relationship, values of *SF* are extracted from the curve-fitting at a null pump–probe delay (continuous lines): 8.5 μJ·cm^{-2} with $A = 0.25$, and 14.5 μJ·cm^{-2} with $A = 0.19$, respectively for surface area 1 and surface area 2 of Mic-SWNT sample.

are considered due to the inhomogeneity of the dropped film (surface area 1 and surface area 2 as indicated in Fig. 3). Figure 3 shows that for a pump fluence of 15 μJ·cm^{-2}, Mic-SWNT film exhibits transient bleaching amplitude 5 to 10 times higher than MQW and B-SWNT according to the surface area under study. The *SF* parameter for Mic-SWNT is much lower as compared to other nanostructures based SA (8.5 and 14.5 μJ·cm^{-2} for area 1 and area 2 with $A = 0.25$ and 0.19, respectively). These results suggest that Mic-SWNT optical response amplitude can be improved by a proper control of the SWNT film thickness. Measurements at higher pump power can be done for B-SWNT and MQW in contrast with Mic-SWNT. Indeed, Mic-SWNT need to be pumped at a lower power level due to the presence of the surfactant around carbon tubes which prevent them to form bundles. Moreover, as compared to fiber mode-locked lasers, which use saturable absorber at high fluence, enhanced nonlinearity at low pump power is suitable for telecom application (especially for signal regeneration).

SF for MQW and B-SWNT cannot be estimated here by curve-fitting with the saturation relationship because the NDT remains linear in this weak pump intensity regime. Previous observations on these nanostructures have shown nonlinear trends for higher excitation intensity dependence.[9] From the NDT maximum value, *SF* of 70 and 726 μJ·cm^{-2} were extracted for MQW and B-SWNT, respectively.[9] Thus using Mic-SWNT film in SA devices improves and reduces the *SF* parameter by a factor of 8 to 90. Previous experiments on band gap photobleaching have already pointed out a similar enhancement by a factor of 2 for Mic-SWNT as compared to B-SWNT.[17] In our case, this enhancement is attributed to the resonance of one Mic-SWNT family with the operating wavelength. As a consequence, absorption in this sample is more easily saturated than in the B-SWNT film where absorption is mainly due to the large background.[8,17] Further improvement can be provided thanks to selective tuning of SWNT films absorption peaks near 1.55 μm using SWNT diameters sorting by the density gradient ultracentrifugation method.[18] But a compromise between the time dynamics, the contrast and *SF* values have to be found as regards to the targeted application (more resonant SWNT imply an exaltation of the long interband dynamics in the case of Mic-SWNT films).[6,8] Let us note that the *SF* results here are very close to the values obtained with Fe doped MQW microcavity in reflection configuration (i.e., 1.9 μJ·cm^{-2}).[19]

In conclusion, transient transmission dynamics of HiPCO B-SWNT and Mic-SWNT deposited on glass substrate have been measured and compared to 40 periods Fe-doped InGaAs/InP MQW. Experimental data have been recorded in the same experimental run. All samples show the same order of recombination time which is between 1 to 2 ps range. Micelles environment of SWNT induce a change on the dynamics of Mic-SWNT in comparison with B-SWNT, but in return both transient bleaching amplitude and *SF* are highly enhanced. The amplitude of NDT for Mic-SWNT is found to be 10 times higher and their *SF* value is improved and reduced by at least a factor of 8. These results suggest that efficient low cost and temperature insensitive SA for AOSR can be achieved by using SWNT in preference to MQW.

1) O. Leclerc, B. Lavigne, E. Balmefrezol, P. Brindel, L. Pierre, D. Rouvillain, and F. Seguineau: J. Lightwave Technol. **21** (2003) 2779.
2) H. Trung Nguyen, J.-L. Oudar, S. Bouchoule, G. Aubin, and S. Sauvage: Appl. Phys. Lett. **92** (2008) 111107.
3) Q. Trung Le, A. O'Hare, N. Hoang Trung, L. Bramerie, M. Gay, G. Aubin, H. Ramanitra, M. Joindot, J. L. Oudar, and J. C. Simon: Opt. Commun. **282** (2009) 2768.
4) M. Guézo, S. Loualiche, J. Even, A. Le Corre, H. Folliot, C. Labbé, O. Dehaese, and G. Dousselin: Appl. Phys. Lett. **82** (2003) 1670.
5) J. S. Lauret, C. Voisin, G. Cassabois, C. Delalande, Ph. Roussignol, O. Jost, and L. Capes: Phys. Rev. Lett. **90** (2003) 57404.
6) L. Huang, H. N. Pedrosa, and T. D. Krauss: Phys. Rev. Lett. **93** (2004) 17403.
7) Y.-C. Chen, N. R. Raravikar, L. S. Schadler, P. M. Ajayan, Y.-P. Zhao, T.-M. Lu, G.-C. Wang, and X.-C. Zhang: Appl. Phys. Lett. **81** (2002) 975.
8) A. Maeda, S. Matsumoto, H. Kishida, T. Takenobu, Y. Iwasa, M. Shiraishi, M. Ata, and H. Okamoto: Phys. Rev. Lett. **94** (2005) 47404.
9) H. Nong, M. Gicquel, L. Bramerie, M. Perrin, F. Grillot, C. Levallois, A. Maalouf, and S. Loualiche: Appl. Phys. Lett. **96** (2010) 61109.
10) M. J. O'Connell, S. M. Bachilo, C. B. Huffman, V. C. Moore, M. S. Strano, E. H. Haroz, K. L. Rialon, P. J. Boul, W. H. Noon, C. Kittrell, J. Ma, R. H. Hauge, R. B. Weisman, and R. E. Smalley: Science **297** (2002) 593.
11) O. J. Korovyanko, C.-X. Sheng, Z. V. Vardeny, A. B. Dalton, and R. H. Baughman: Phys. Rev. Lett. **92** (2004) 17403.
12) Y.-Z. Ma, L. Valkunas, S. M. Bachilo, and G. R. Fleming: J. Chem. Phys. B **109** (2005) 15671.
13) D. Södertröm, S. Marcinkevicius, S. Karlsson, and S. Lourdudoss: Appl. Phys. Lett. **70** (1997) 3374.
14) M. Guézo, S. Loualiche, J. Even, A. Le Corre, O. Dehaese, Y. Pellan, and A. Marceaux: J. Appl. Phys. **94** (2003) 2355.
15) L. Qian, S. D. Benjamin, P. W. E. Smith, B. J. Robinson, and D. A. Thomsen: Appl. Phys. Lett. **71** (1997) 1513.
16) D. S. Chemla, D. A. B. Miller, P. W. Smith, A. C. Gossard, and W. Wiegmann: IEEE J. Quantum Electron. **20** (1984) 265.
17) M. S. Arnold, J. E. Sharping, S. I. Stupp, P. Kumar, and M. C. Hersam: Nano Lett. **3** (2003) 1549.
18) M. S. Arnold, A. A. Green, J. F. Hulvat, S. I. Stupp, and M. C. Hersam: Nat. Nanotechnol. **1** (2006) 60.
19) M. Gicquel-Guézo, S. Loualiche, J. Even, C. Labbé, O. Dehaese, A. Le Corre, H. Folliot, and Y. Pellan: Appl. Phys. Lett. **85** (2004) 5926.